Made available by Hasselt University Library in https://documentserver.uhasselt.be

Performance of Zigzag Photovoltaic Noise Barriers near a Belgian Highway

Peer-reviewed author version

BOUGUERRA, Sara; DE JONG, Richard; Le, Philip; Di Giusto, Fabio; Colberts, Fallon; KAAYA, Ismail; CASASOLA PAESA, Marta; MORLIER, Arnaud; Deckers , Elke; KYRANAKI, Nikoleta & DAENEN, Michael (2024) Performance of Zigzag Photovoltaic Noise Barriers near a Belgian Highway. In: Solar RRL,.

DOI: 10.1002/solr.202400519
Handle: http://hdl.handle.net/1942/44547

Performance of Zigzag Photovoltaic Noise Barriers in a Belgian Highway

Sara Bouguerra, Richard De Jong, Philip Le, Fabio Di Giusto, Fallon Colberts, Ismail Kaaya, Nikoleta Kyranaki, Marta Casasola Paesa, Elke Deckers, Arnaud Morlier, Michaël Daenen*

S. Bouguerra
Institute for Materials Research (IMO), Hasselt University, Diepenbeek, Belgium
Imec, Imo-Imomec, Thor Park, Genk, Belgium
EnergyVille, Genk, Belgium
E-mail: sara.bouguerra@uhasselt.be

R. De Jong, I. Kaaya and A. Morlier
Imec, Imo-Imomec, Thor Park, Genk, Belgium
EnergyVille, Genk, Belgium

P. Le, F. Di Giusto and E. Deckers
Department of Mechanical Engineering, KU Leuven, Celestijnenlaan 300 B, B-3001 Heverlee, Belgium
Flanders Make@KU Leuven, B-3001 Heverlee, Belgium
Department of Mechanical Engineering, KU Leuven, Campus Diepenbeek, Wetenschapspark 27, 3590 Diepenbeek, Belgium

F. Colberts
Zuyd University, Heerlen, The Netherlands

N. Kyranaki, M. Casasola Paesa and M. Daenen
Institute for Materials Research (IMO), Hasselt University, Diepenbeek, Belgium
Imec, Imo-Imomec, Thor Park, Genk, Belgium
EnergyVille, Genk, Belgium

Keywords: Solar energy, noise barriers, PVNB, energy yield, modelling

In this study, the energy performance of photovoltaic noise barriers (PVNBs) with cassette built-on and shingles built-on design is evaluated using imec's energy yield framework. The simulation is validated through on-site electrical and thermal measurements, then, the same design is employed for a case study near E19 road in Belgium using different scenarios. To optimize the energy yield, variations in the noise barrier height, orientation, and PV module tilt are introduced. The energy yield is then simulated to identify the optimal combination of parameters to maximize energy production. The results show that the cassette built-on PVNB with fixed cassette distance provides higher energy yield throughout the year compared to other scenarios, and a low-rise noise barrier is more energy efficient due to reduced shading effects. Sound pressure simulation conducted in COMSOL reveals that the cassette built-on and shingles built-on have comparable performance in sound reduction, and high-rise noise barriers with small tilts (20° to 40°) are optimal for sound pressure attenuation.

1. Introduction

According to Statbel,[1] the Belgian statistical office, 72% of the Belgian population resides within 5 kilometers from a motorway entrance. In the province of Liège, for example, 31% of the population lives within 1 kilometer of a motorway. In densely populated areas, noise barriers play a crucial role in mitigating the adverse effects of traffic-related sound pollution. These barriers serve as effective tools to enhance the quality of life for residents, providing a shield against the noise generated by constant vehicular activity. Different factors need to be considered in the design of a noise barrier, mainly the acoustical and non-acoustical considerations. The acoustic performance of noise barriers varies depending on their material and surface treatment. Some of the original noise energy is reflected or scattered back toward the source, while other portions are absorbed by the barrier material, transmitted through it, or diffracted at its top edge. The transmitted noise reaches the receiver with certain loss of acoustical energy, as some energy is redirected, and some is converted into heat. This reduction in noise energy is expressed in decibels (dB) and is called the Transmission Loss (TL), which is the energy ratio between the noise in front of the barrier and behind it. The TL is affected by the barrier material, its thickness, surface density, and the frequency spectrum of the noise source. Non acoustical considerations include vehicular impact, fire resistance, emergency exists and ventilation, etc.[2] Photovoltaic Noise Barriers (PVNB) offer a dual-purpose solution by combining the benefits of noise reduction with the generation of solar energy. The first PVNB was built in Switzerland in 1989. The PV plant is constructed on top of an existing sound-barrier structure along the A13 motorway in the Swiss Alps, with a capacity of 100 kWp.[3] Currently, the predominant approach for PVNBs focuses on the top-mounted design, which facilitates the expansion of the surface area of pre-existing noise barrier structures.

The construction of these barriers involves a diverse range of materials, including but not limited to concrete, earth, wood, glass, and metal.[4]

Nowadays, with the massive decline in the cost of PV modules, 90% since 2000[5], PV noise barriers with shingle and cassette configurations become a remarkable solution in the design of PVNBs. Their distinctive feature lies in the flexibility they offer in terms of design and accommodation of various sizes and shapes.[6]-[7] Furthermore, the PV panels integrated into the noise barrier with cassette technology uses a combination of sound reflection and sound absorption. Additionally, they can be precisely configured to align with diverse energy requirements. Sound absorption is enabled through integrating noise absorbing material into the zigzag cassettes to reduce undesired reflection of traffic noise by concrete walls.[8]

In ref. [6], the energy production from PVNB systems was estimated across the US for different PV module tilts and orientations. In ref. [9], the energy output of various PVNB configurations, such as vertical built-on, shingles built-on, and top-mounted designs, was evaluated with different scenarios (tilts, orientations, number of shingles..). In another study,[10] the energy performance of different noise barrier demonstrators with several configurations (top-mount, cassettes and rear-side integrated) is compared utilizing different noise absorber types. To the authors best knowledge, comprehensive energy yield and sound pressure simulation has not been conducted yet for PV noise barriers utilizing the zigzag configuration with cassettes. This study aims to address this gap by thoroughly examining the PV energy performance and noise reduction capability of the noise barrier with this specific design and compare it with the conventional design of shingles. A case study is evaluated in the European road E19 in Kontich, Antwerp, Belgium to explore the impact of noise barrier height, module tilt, orientation angle and cassette dimensions on the yearly energy yield and noise reduction capability for this specific location, renowned for its high traffic volume. The originality of this study lies in the detailed energy yield assessment of cassettes and shingles built-on PVNBs with acoustic performance. This article examines the influence of various design parameters such as cassette/shingle configuration, tilt, orientation, and barrier height on both energy output and noise reduction capability, aiming to identify the optimal design parameters that enhance both aspects based on relationship between the two. The methodology and data presented in this paper will assist architects, researchers, and policymakers in optimizing the energy yield of shingles and cassette built- on noise barriers in locations with similar climate conditions. The acoustic pressure simulations will assist in optimizing the noise reduction as well (by reflection or absorption).

Due to the complexity of PVNB geometry, an advanced simulation tool developed by imec is utilized. This simulation tool calculates energy yield with high precision as it considers the reflection of light from the ground and plane of array irradiance influenced by module frames, system components' geometry (cassettes, concrete wall) and varying albedo, and the thermal model in the framework incorporates a heat transfer model which considers the noise absorbing material embedded into the zigzag cassettes. A 2D acoustic simulation is conducted in COMSOL to simulate the acoustic pressure and quantify the noise attenuation caused by noise barriers with cassette and shingles built-on designs on the receptor side.

2. Methodology

2.1. IIPV demonstrator

In the context of the SolarEMR project,[11] a PVNB demonstrator was built in Chemelot Campus in Geleen, comprising a 4-meter-high and 4-meter-long south-facing concrete wall. Two zigzag configurations were built adjacent to each other, each comprising four cassettes. All cassettes are filled with noise-absorbing material[12] to mitigate the undesired reflection of traffic noise by the concrete walls. Eight customized glass/glass PV modules from Soltech (103 W each) are placed on the cassettes and connected in series, forming two strings—one on the east side (String A) with PV modules tilted at 35° from the horizontal and one on the west side (String B) with module tilt of 50°, as shown in **Figure 1,** the PV module datasheet is given in **Table 1** (electrical model) in the **supporting information**.

The PV strings are connected to a DC/AC converter with four Maximum Power Point (MPP) inputs (APS YC100-3), which feeds the AC electricity into the grid. The DC power generated is monitored by a QEED QI-power-485-LV, measuring current at MPP (Impp), voltage at MPP (Vmpp), and power at MPP (Pmpp) every 2 minutes. The temperature of each solar panel is recorded using DS18B20 temperature sensors attached to the back of the panels. The weather station (Lambrecht Meteo EOLOS-IND) is equipped with a pyranometer, temperature sensor, and wind sensor installed at the Brightlands Chemelot Campus in Geleen. Additionally, Fiber Bragg Grating (FBG) sensors are installed on the bottom left and right panels to monitor the temperature of the silicon wafers from May 2023 to present. A 4-channel DM-4120 Sentea interrogator was used with a sampling frequency of 0.1 Hz to monitor the wavelength variations of the FBG sensor. The wavelength values can be visualized via an InfluxDB account. Then, they are converted into the corresponding temperature values in degrees Celsius by using a 2nd-order polynomial obtained from the calibration of the temperature sensors in a climate chamber. Further details on the FBG temperature sensors can be found in ref.[13]. A paper on the configuration of the PV system (interconnection, different materials used) with life cycle assessment (LCA) study is being published in parallel.

Figure 1 Noise barrier demonstrator.

2.2. Energy Yield simulation

To accurately evaluate the PVNB performance, an advanced bottom-up physics-based energy yield simulation framework[14] was deployed. The simulation framework integrates detailed optical, thermal, and electrical models to closely mimic realistic operational conditions, providing a dynamic analysis of system performance under various scenarios. A flowchart of the energy yield simulation framework is shown in the **supporting information**.

- **Geometrical modelling**: The PV plant 3D geometry is created using an inhouse scene generator tool developed in python. A virtual environment is created based on different elements: modules, cells and structural elements such as the concrete wall, zigzag cassettes and shading elements. Each element is given parameters such as length, width, azimuth, and tilt. General functions enabling the translation, rotation, equal spacing, alignment and grids are developed to chain up the elements and create a single or multiple scenes. A 3D model created using the scene generator for a 6 m high noise barrier is shown in the **supporting information**.
- **Optical modelling**: The framework includes a ray tracing model[15], which simulates the path of solar rays as they interact with PV elements. By tracing the trajectory of individual rays through the atmosphere and considering factors such as cloud cover, shading, and atmospheric conditions, the model provides a precise estimation of plane

of array (POA) irradiance using irradiation components such as the global horizontal irradiance (GHI), diffuse horizontal (DHI) and direct normal (DNI).

- **Thermal Modelling:** The thermal model used in imec simulation framework is represented by an equivalent resistor-capacitor (RC) circuit where the equivalent thermal resistances and capacitors are computed on each layer of the PV module. Thermal irradiation and convective cooling of the module surfaces are modelled by means of input-dependent thermal resistors, which may have time-varying, highly non-linear properties. Solving the circuit enables the computation of heat conduction within the layered structure and this increases the accuracy of cell temperature calculation.
- **Electrical Modelling:** The electrical model uses the single diode equation with a temperature dependent diode, series, and shunt resistances, providing high accuracy at acceptable computational costs. The coupling between the thermal and electrical models is established by considering the net power absorbed in the solar cell (provided by the optical model). Some part of this power is extracted from the solar cell in the form of electrical power and the other part is converted into heat and injected to the thermal network by a current source in the solar cell layer of the thermal RC network. These heat transfer processes influence the solar cell temperature, which affects the temperature dependent diode, consequently altering the extracted electrical power.

2.3. Simulation Scenarios

The simulated electrical performance of the PVNB demonstrator is validated using performance monitoring on site. Then, the same design is adopted to simulate a case study in Belgium, near the highway E19, the areal and street view of the road is provided in the **supporting information**. In this simulation, the noise barrier dimensions are slightly modified to integrate more PV modules and study different scenarios, details of the optical, electrical and thermal properties utilized in the Energy yield framework are shown in **Table 1** in the **supporting information**, the thermal properties for glass, encapsulation, and silicon cells are not detailed there, as the simulation uses default values commonly found in the literature.

To evaluate the impact of module tilt, noise barrier height and orientation on the yearly energy yield, the scenarios in the simulation include:

- **Scenario 1 (S1):** Cassette built-on PVNB with fixed cassette distance, the height of the zig-zag structure (cassette) in the vertical axis is fixed to 0.71 m and the zag length is varied to accommodate different tilt angles (20°, 25°, 30°, ...80°), as shown in **Figure 2 (A)**.

- **Scenario 2 (S2):** Cassette-built-on PVNB with variable cassette height and fixed zig-zag ratio: In this case, the zig length is made equal to the zag length (module width), which is 0.441 m as shown in **Figure 2 (B)**. For this scenario, the number of rows in the noise barrier varies according to the tilt angle. Smaller tilt angles will allow more cassettes to be attached to the wall.
- **Scenario 3 (S3):** shingles-built on PVNB with fixed shingle distance: in this case, PV modules are mounted as shingles on the surface of the barrier without cassettes, as depicted in **Figure 2 (C)**.

For each scenario, the concrete wall is positioned to have west orientation, aligned with the road's trajectory. south orientation is also tested for comparison. The PV modules tilt is varied from 20° to 80° and the height of the wall is set at 4 m, 6 m, and 8 m to evaluate the sensitivity of tilt angle to wall height for optimization purpose. Yearly energy yield simulations are then conducted using the E-Yield framework to determine which combination of parameters (PVNB configuration, tilt and height) optimizes energy yield at the selected location. The shading effect from overhead cassettes (in S1 and S2) and from the overhead shingle structures (in S3), is considered in the POA irradiance estimation by the raytracing tool in the framework and, thus, considered in the energy yield evaluation. Typical Meteorological Year (TMY) for the region of Kontich, E19 Antwerp are collected from the PVGIS database[16] to carry out the simulation.

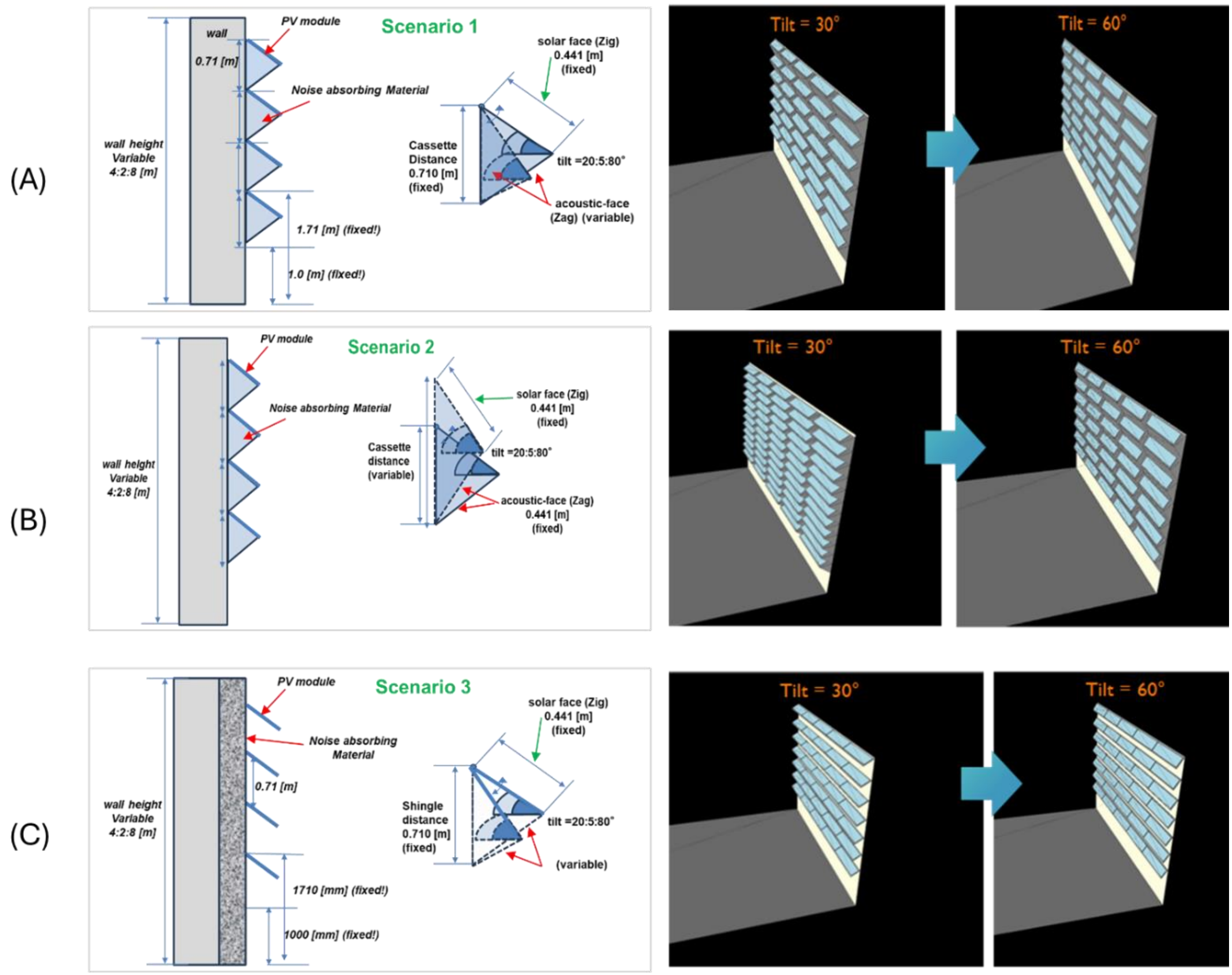

Figure 2 Simulation scenarios with scene generator view, (A) Cassette built-on noise barrier with fixed cassette distance, (B) Cassette built-on noise barrier with variable cassette height and fixed zig-zag ratio and (C) shingles built-on noise barrier with fixed shingle distance.

To implement the PV plant in the Energy Yield framework, horizontal stringing is adopted, where each row of modules is connected to a single maximum power point tracking (MPPT). The number of MPPTs is equal to the number of rows in the PVNB. This setup minimizes losses due to shading by the overhead cassettes in Scenarios 1 and 2, and by the upper modules in Scenario 3. A noise barrier geometry with zigzag design was constructed in the scene generator tool, the PV system consists of 5 modules per row, and the number of rows is determined by the height, the cassette distance and the scenario studied, as shown in **Figure 2**. To remove the boundary conditions effect in the results interpretation, the two corner modules are excluded from the energy yield calculation. However, they are still considered in the evaluation of plane of array irradiance to account for shading effects. Only the three middle modules are considered for the energy yield calculation and are connected to a single MPPT in each row.

2.4. Acoustic Pressure Simulation

A 2D geometry model for the PV noise barrier is constructed in COMSOL using S1: cassette PVNB with fixed cassette distance, and S3: shingles PVNB with fixed shingle distance, see **Figure 3**. The simulations assume the following conditions:

- Noise from vehicles is modelled as a 'Monopole' (point source radiating sound equally in all directions) with a unit amplitude.
- In the cassette-built on case, the aluminium cassettes are perforated and filled with a poroelastic material and modelled as an equivalent fluid model (EFM).
- For the shingles wall (S3), an absorbing boundary condition was selected on the surface of the wall (absorbing class 4).
- Perfectly matched layers are added on the boundaries of the free field domain to model the open and non-reflecting infinite domain.
- The asphalt (ground) and concrete wall with thickness of 0.3m are modelled as rigid (complete reflection of sound at boundary).

A monopole noise source is placed 2.75 meters from the barrier, and 4 different microphones are placed 30 m and 50 m meters from the noise source in two directions, in front of and behind the wall, the two distances were chosen based on the Roads and Traffic Agency in Belgium.[17] The noise source is 0.5 meters above the ground, and all microphones are placed 2 meters above the ground. Two heights for the wall are simulated, 4 and 8 meters, and the tilt angle of the PV modules is varied from 20° to 60° with a step size of 10°. According to the studies[18]-[19], the frequency of traffic noise falls in the range of 500 Hz–2500 Hz, hence, for this study the sound pressure level in dB is simulated for frequencies from 100 Hz to 2500 Hz.

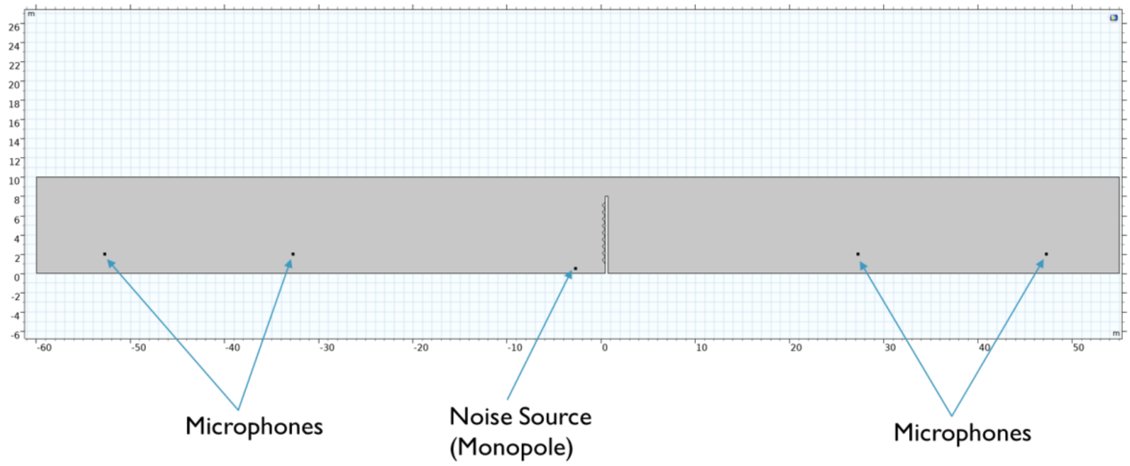

Figure 3 Geometry model in COMSOL for cassettes built-on PVNB with 8m height.

3. Results and Discussion

3.1. Validation of the Energy Yield model using cassette built-on demonstrator

For validation of the noise barrier performance, the meteorological data (GHI, ambient temperature, wind speed and wind direction) are measured onsite in Chemelot Campus and employed for simulations. The DNI and DHI are obtained using decomposition models.[20]-[21] **Figure 4** presents a comparison between the simulated and measured power at MPP for the string (A), and string (B), respectively (see **Figure 1**) in the noise barrier demonstrator in August 2023. It can be observed that the measured and simulated power profiles are aligned with each other for the right string (string A), while for the left string (String B), the measured power slightly exceeds the simulated power, which is attributed to a slight overestimation of cell temperature in the simulation (see **Figure 5**). For both strings, Root Mean Square Error (RMSE) is around 19W. **Figure 4** also shows that the modules on the east side, inclined at 35°, typically produce less energy compared to their counterparts on the west side (tilted at 50°), this is due to the shading effects on the lower modules by the overhead cover.

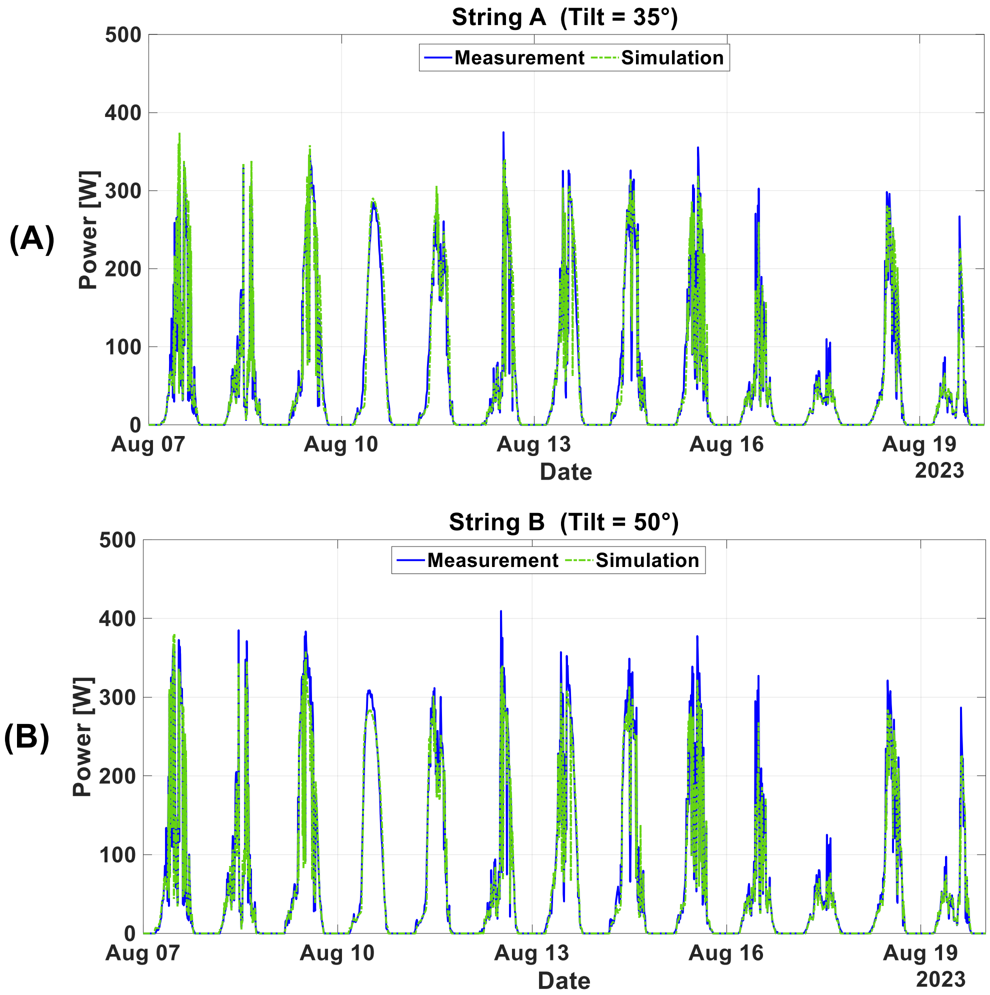

Figure 4 Measured VS simulated power at MPP for the noise barrier demonstrator, (A) for string A and (B) for string B.

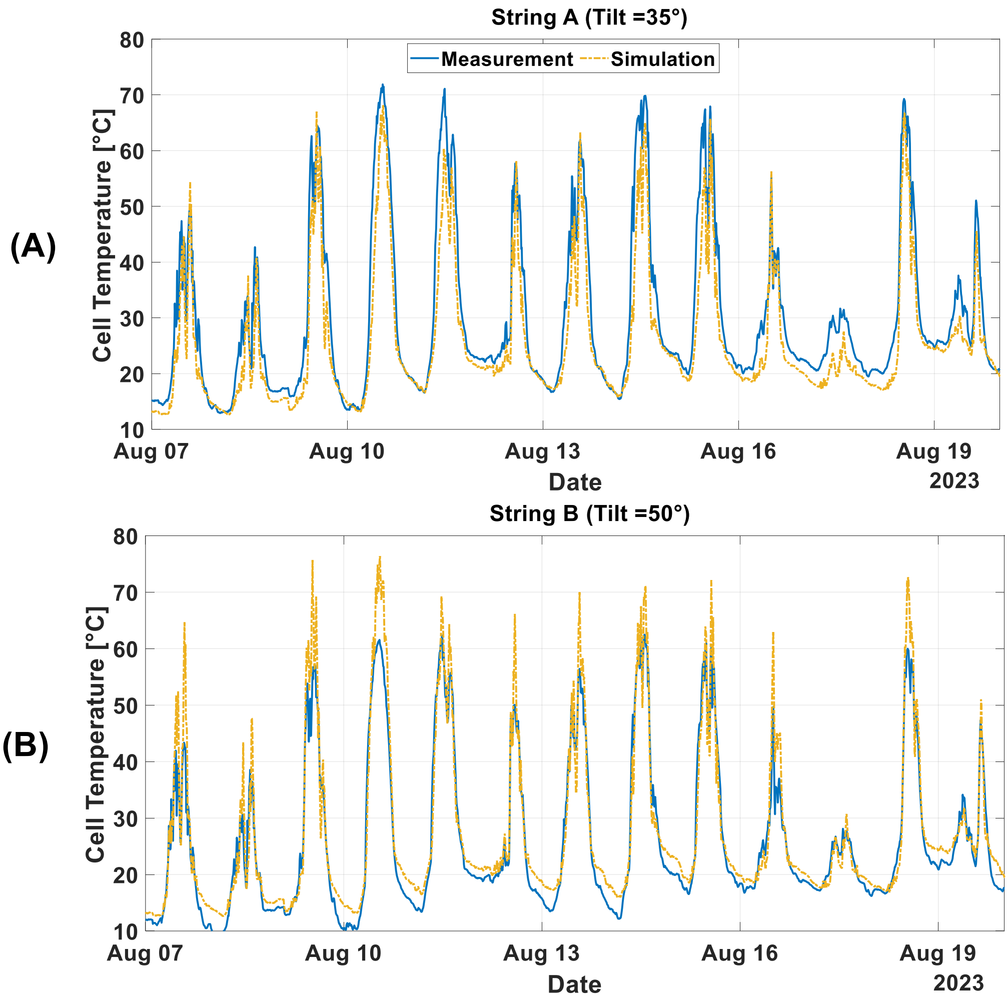

Figure 5 Measured VS simulated cell temperature (in bottom modules) for the noise barrier demonstrator, (A) for string A and (B) for string B.

Measured and simulated cell temperature for the bottom modules of String A and String B are shown in **Figure 5**. It is noted that the temperatures are generally consistent, except for String B at noon, this discrepancy is most likely due to the complexity of the thermal model and the modelling of the noise-absorbing material (Rockwool) in the simulation.

3.2.Energy Yield simulation

3.2.1 Energy Yield Scenario 1

Figure 6 illustrates the annual specific yield in kWh/ kWp of the PV noise barrier located in Kontich, Antwerp near highway E19 for three different heights: 4, 6 and 8 meters and using module tilt angles ranging from 20° to 80° for scenario 1. The results are shown for two orientations, west and South.

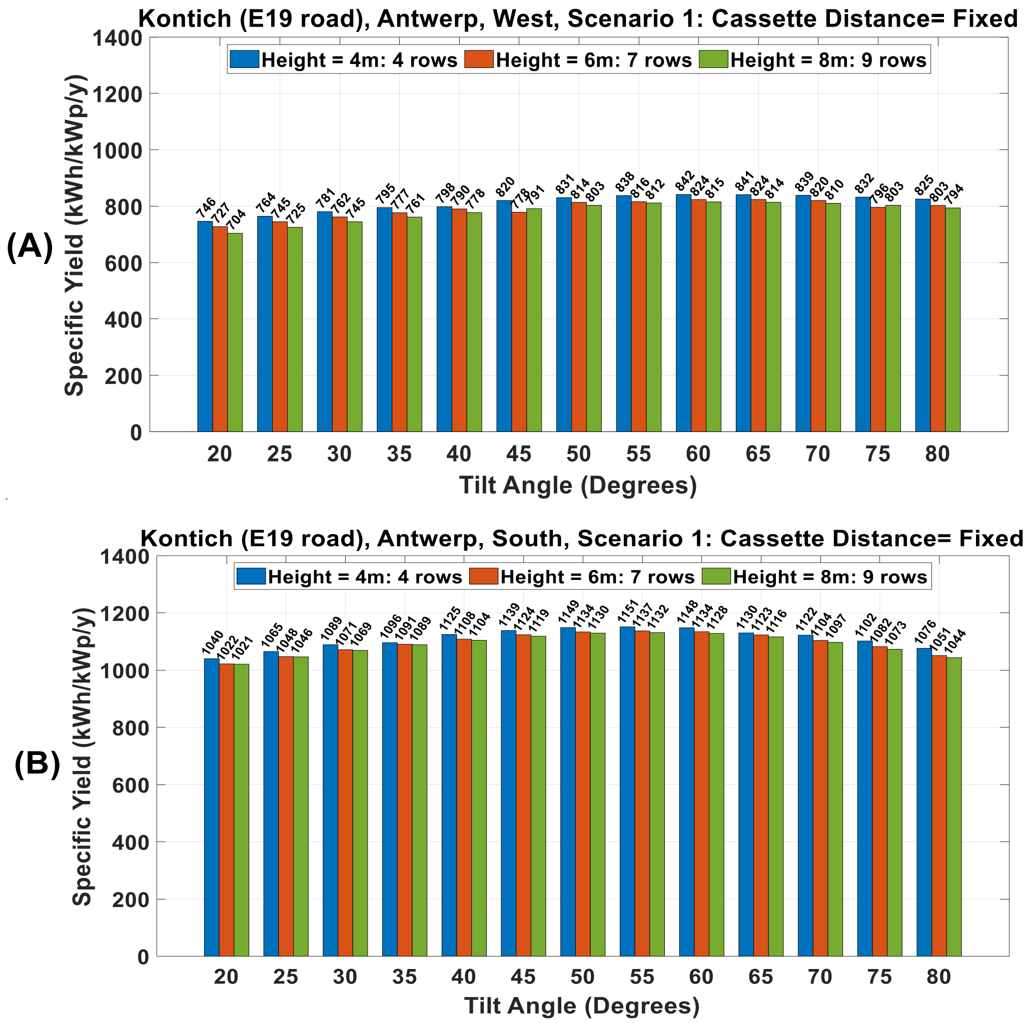

Figure 6 Specific Yield for the noise barrier in E19 for scenario 1: cassette PVNB with fixed cassette distance for (A) West orientation, (B) South orientation.

It can be observed from **Figure 6**, that the highest specific yield using scenario 1 for the different noise barrier heights is achieved with south orientation, wall height of 4 m and tilt angle 60°. The orientation loss is around 30% and the specific yields for different tilts remain within a range of 13% below the optimum for west facing, and 10% for south orientation.

3.2.2. Energy Yield Scenario 2

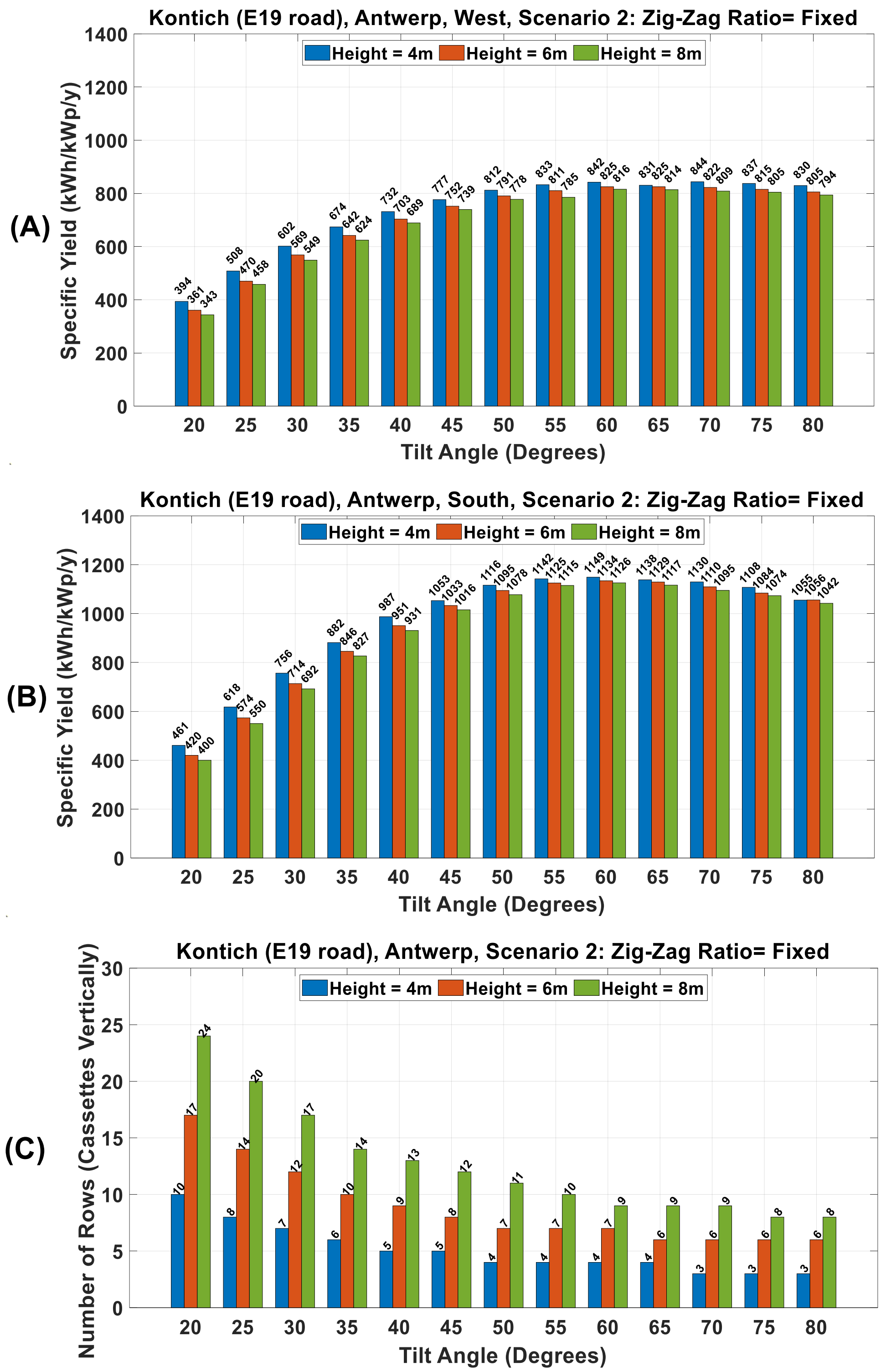

Figure 7 Specific Yield for the noise barrier in E19 for scenario 2: cassette PVNB with fixed zig-zag ratio for (A) West orientation, (B) South orientation, (C) number of rows (cassettes in the vertical direction).

Figure 7 (A) and **Figure 7 (B)** illustrates the specific yield for scenario 2, cassette built-on PVNB with fixed zig-zag ratio. It can be remarked that for both orientations (west and south), the specific yield drops significantly for tilt angles between 20° and 45° (by 8% to 64%, respectively). This is due to the increased shading from the higher number of stacked cassettes along the wall when using small (shallow) tilt angles for the modules, as shown in **Figure 7 (C)**. For tilts between 50° and 80°, the specific yield is comparable to Scenario 1 (with a difference of less than 50 kWh/kWp).

3.2.3. Energy Yield Scenario 3

The specific yield in scenario 3, shingles built-on PVNB with fixed shingle distance is shown in **Figure 8**.

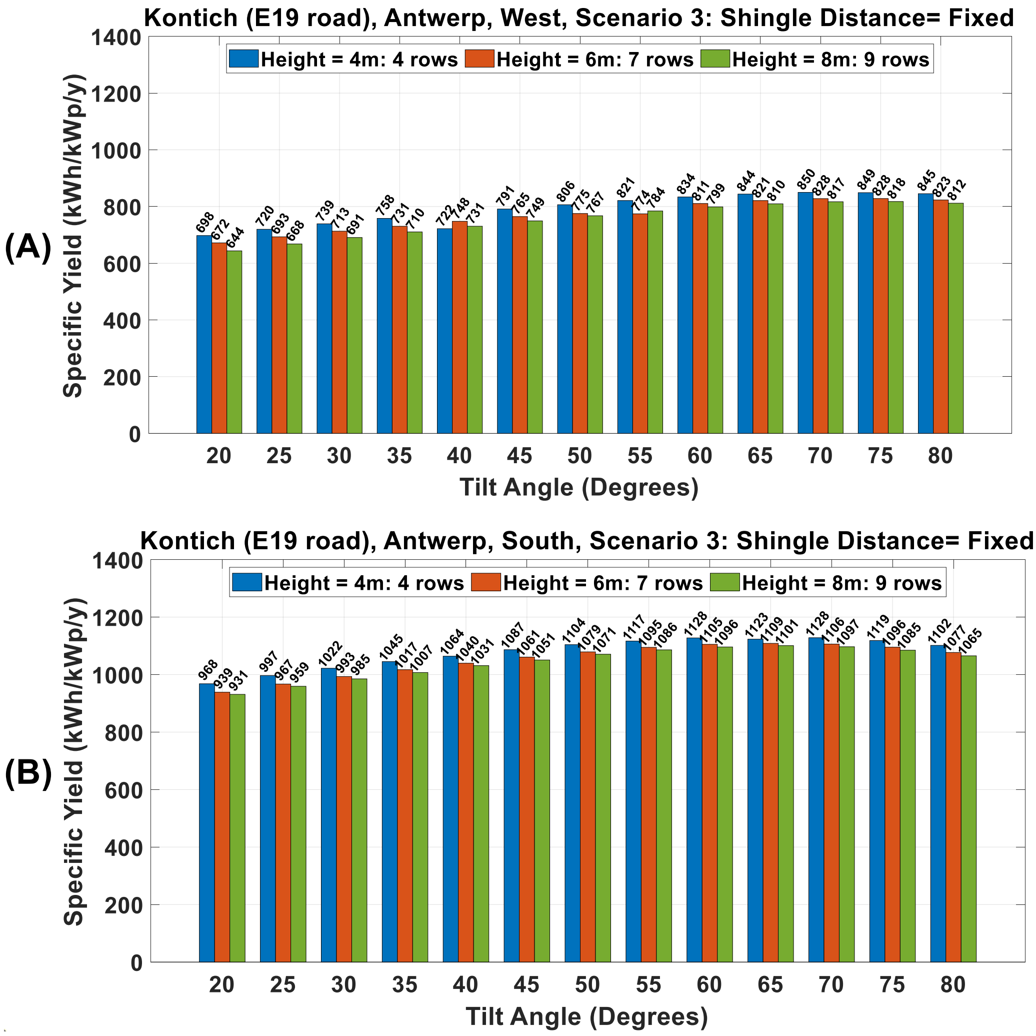

Figure 8 Specific Yield for the noise barrier in E19 for scenario 3: Shingles built-on with fixed shingle distance for (A) West orientation, (B) South orientation.

It can be observed from **Figure 8**, that the optimum yield throughout the year for this scenario is obtained with 4 m PVNB and a tilt angle of 70°-75° for west orientation and 60°-70° for south orientation. The specific yield is slightly lower than Scenario 1. This is most likely attributed to less reflected irradiance with shingles, compared to Scenario 1 with aluminum cassettes. Similar to Scenarios 1 and 2, the specific yield decreases as the height of the barrier increases, primarily due to increased shading effects (more modules being shaded by the overhead cassette or shingle). To visualize this effect, the yearly anergy yield per string (MPPT) is shown for scenario 1 and 3 in **Figure 9**, as discussed previously, each row of modules is connected to one MPPT input, the strings are presented from bottom (S1) to top (S9). It can be observed that in both scenarios, the modules on the bottom rows generate less energy annually compared to those on the top row. This is attributed to the shading effects on the bottom rows caused by the overhead cassettes or shingles. This difference is more significant in S3 due to fewer reflections. However, the annual yield for the bottom strings increases significantly when the tilt angle is increased, as the shading effect is reduced.

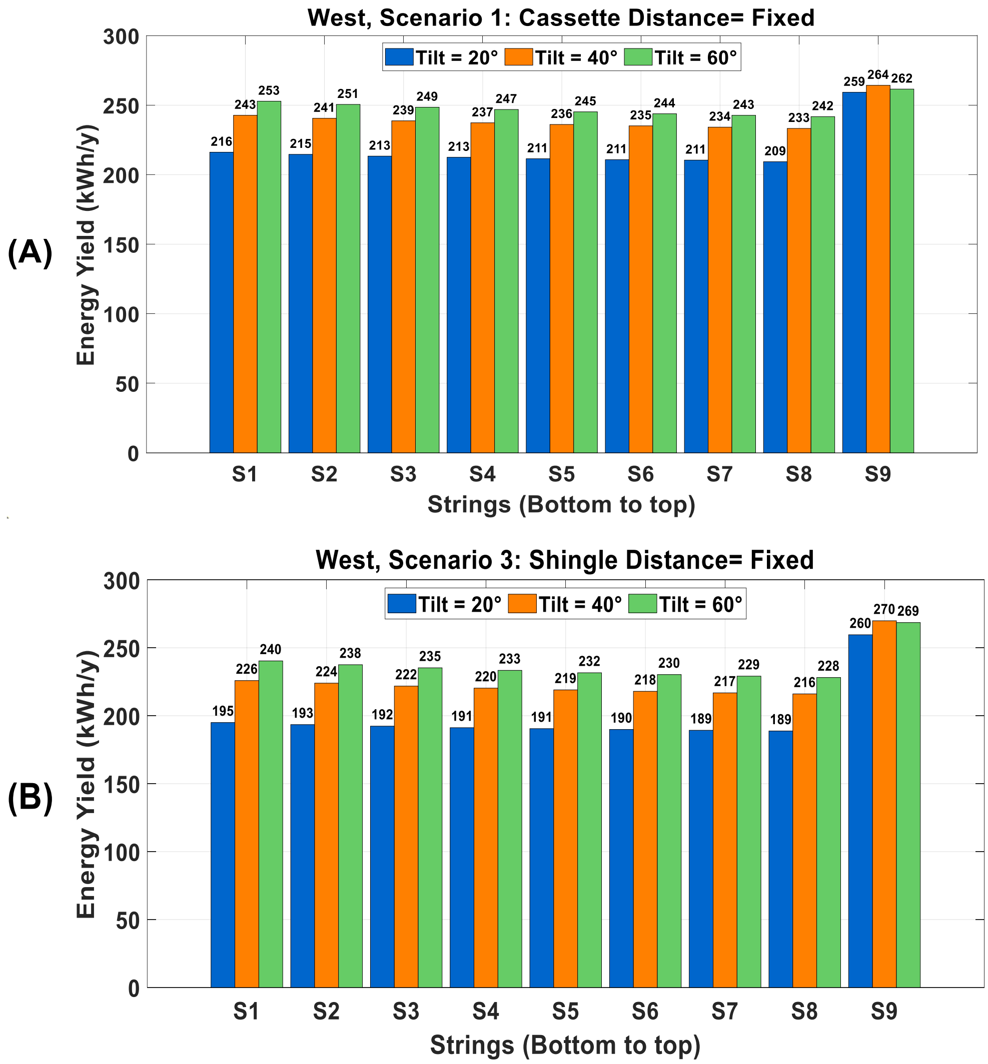

Figure 9 Energy per string (row of 3 modules) for S1 (cassette-built on with fixed cassette height) and S3 (shingles built-on with fixed shingles distance).

Yield per length for scenarios 1, 2 and 3 with west and south orientation is calculated and given in the **supporting information**. It can be remarked that scenario 2 yields the highest energy yield per length through the year, due to the increased number of modules (higher peak power). Comparison between scenarios 1 and 3 reveal that scenario 1 results in a higher energy yield per length due to the reflected irradiance from the cassettes.

To explore this effect, the daily irradiation for Scenario 1 and Scenario 3, with a tilt angle of 60° and a height of 8 m are shown in **Figure 10 (A)**. It can be observed that the daily irradiation varies significantly within the month, especially in summer (May to September) and it is generally higher for the cassette built-on noise barrier case (S1) compared to shingles built-on (S3), the average difference is 1.4 kWh/m² throughout the year, increasing to up to 4 kWh/m² in summer. To visualize the impact of noise absorbing material and its placement on the module temperature for scenarios 1 and 3, **Figure 10 (B)** shows a boxplot representation of average daily module temperature including nighttime temperature for the same scenarios in **Figure 10 (A)**. It can be observed that module temperature in the cassette built-on case is generally higher than the shingles built-on case, this is mainly attributed to noise absorbing material (Rockwool) embedded onto the aluminum cassettes, the difference including nighttime temperature reaches 12°C in summer. The reason for this is that the shingles built-on noise barrier enables more ventilation to the PV modules, resulting in lower module temperature. Despite this effect, the higher module temperatures in the cassette built-on scenario had minimal impact on power performance. Instead, the reflection from the aluminum cassettes significantly influenced energy yield.

(A)

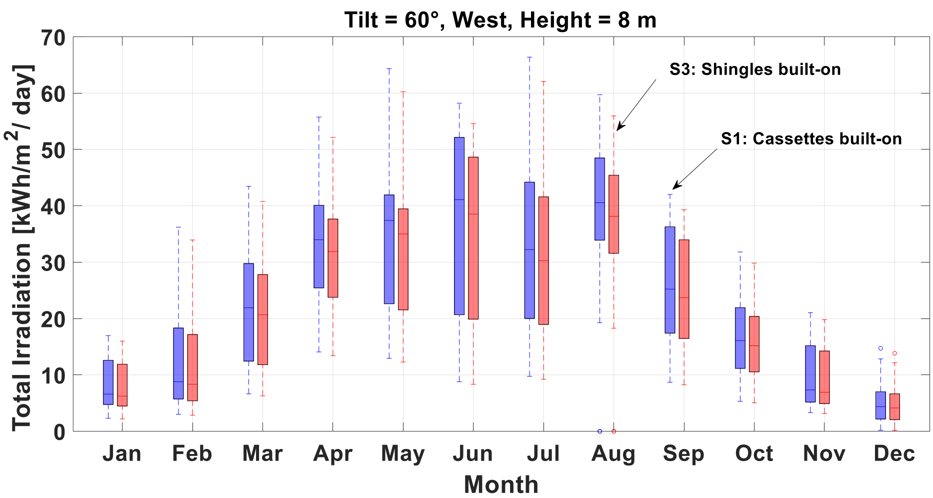

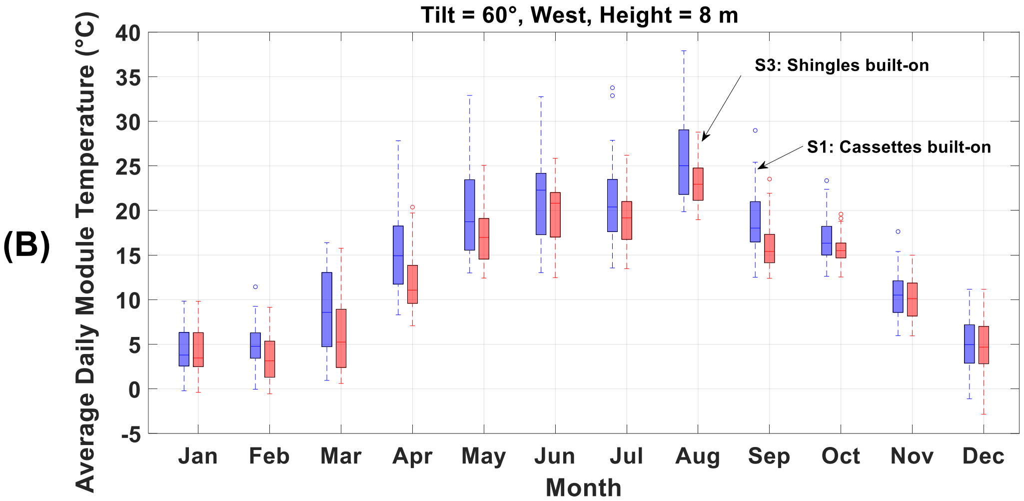

Figure 10 Boxplot showing (A) the total daily irradiation (across all the modules) per month, and (B) average daily module per month for Scenario 1 (Cassette built-on) and Scenario 3 (Shingles built-on), nighttime temperatures are considered in the graph.

3.3. Sound Pressure Results

The total sound pressure for the cassettes built-on and shingles built-on noise barriers with heights of 4 m and 8 m, and frequency of 1000 Hz are shown in **Figure 11**.

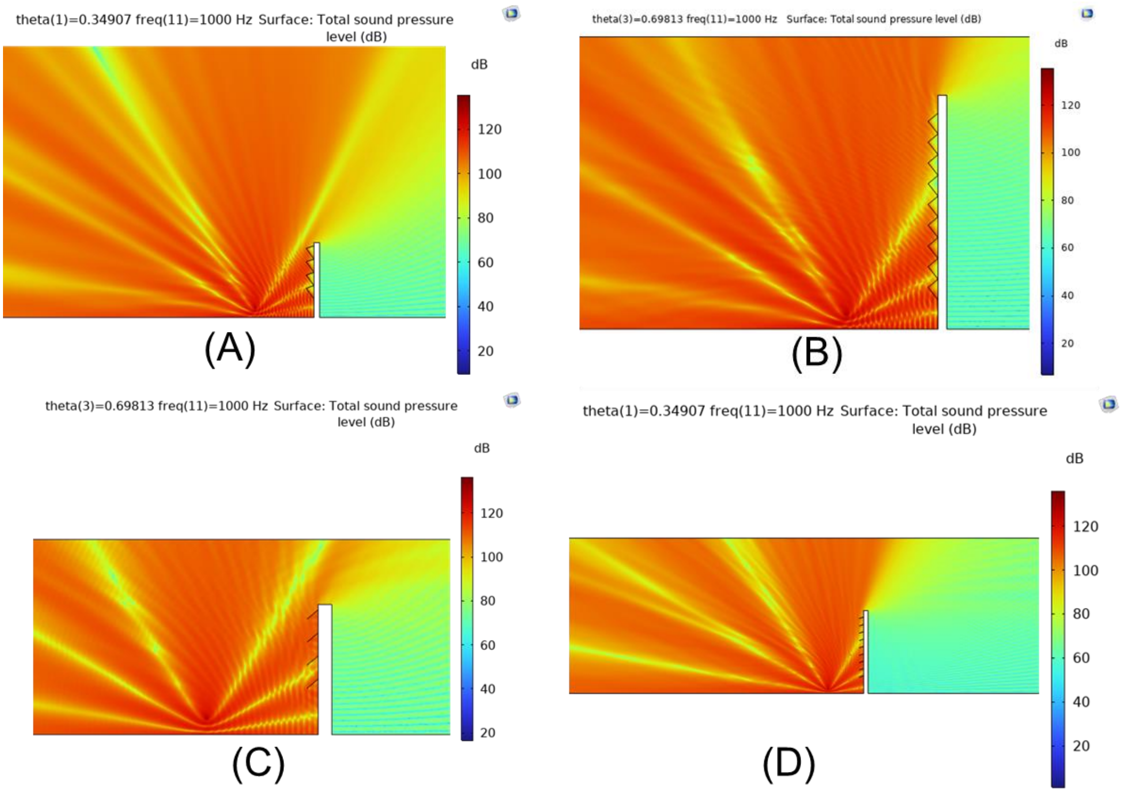

Figure 11 Acoustic pressure and sound pressure level (SPL) for the cassettes built-on noise barriers at 1000 Hz: (A, B) at 4m height and (C, D) at 8m height.

It can be observed from **Figure 11** that the acoustic waves emitted by the cars diffract at the barrier and a taller noise barrier leads to weaker diffracted waves reaching the other side. It is also remarked that the cassette-built on noise barrier can be more effective in noise reduction compared to the shingles built on in the road's side (noise source) due to the reflection of noise at the cassettes which interfere with the reflection from the ground.

Similar to the energy yield analysis, the impact of noise barrier design (shingles, cassettes), height of the barrier and module tilt angle on the acoustic pressure is also studied. The results of Sound Pressure Level (SPL) recorded by a microphone located at 30m for 4 m and 8 m high noise barriers in the receptor side are shown in **Figure 12 (A)** and **(B)**, respectively.

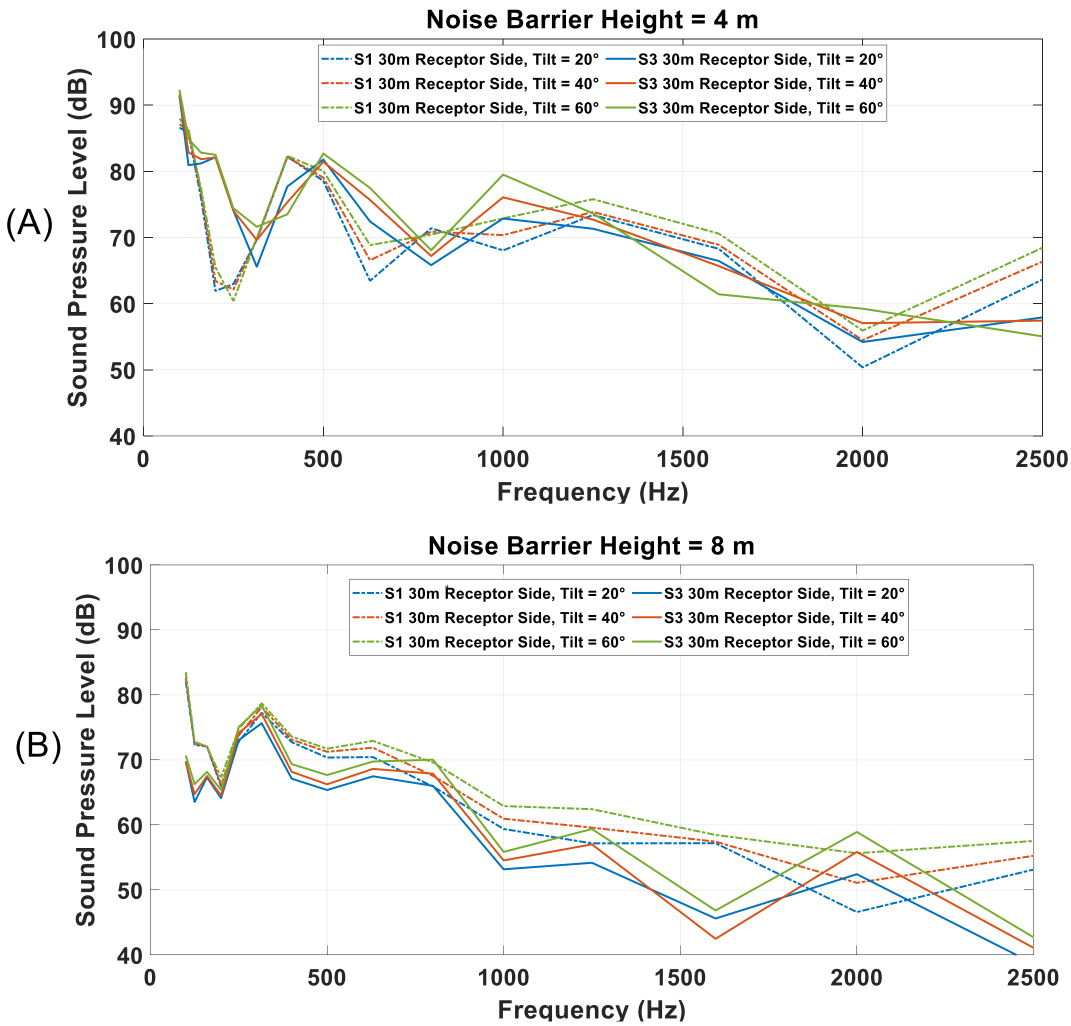

Figure 12 Sound pressure levels recorded by a microphone located at 30m in the receptor side for (A) 4 m high noise barrier, (B) 8 m high noise barrier.

The results show that for a frequency of 1000 Hz, the sound pressure on the receptor side decreases with increased height. For a cassette-built noise barrier with a tilt angle of 20°, the sound pressure is attenuated by 35 dB on the receptor side for a barrier height of 4 meters, and by 43 dB for a height of 8 meters. For a shingle-built noise barrier, the attenuation is 31 dB and 51 dB, respectively, at these heights. The noise reduction capability of the two designs varies with the noise frequency and height of the barrier. The results can also be influenced by the different absorption properties of the barriers (perforated aluminum filled with poroelastic material) in S1 and class 4 absorber in S3.

The sound pressure recorded by the microphone located at 30m in the source side and the microphones located at 50 m in both sides is provided in the **supporting information**.

For both configurations, cassettes (S1) and shingles (S3), the impact of the tilt angle on sound pressure is minimal on the roadside but significant on the receptor side. For the microphone located at 30 m, when the tilt angle changes from 20° to 40° and from 40° to 60°, the sound pressure on the receptor side increases by 1.3 dB to 3 dB. This difference is more pronounced at lower heights.

The acoustic simulation indicates that high-rise noise barriers with low PV module tilt angles (20° to 40°) are more effective at reducing noise. However, energy yield analysis (Section 3.2) shows that as barrier height increases, the specific yield decreases due to shading from overhead cassettes or shingles, while the tilt angle has only a minor impact on annual yield. A balanced solution can be achieved by using moderate-height barriers (around 6 meters) with a low tilt angle (20° to 40°) to optimize both noise reduction and energy output.

The energy yield simulation resulted in accurate predictions of energy yield for the two configurations of PVNBs with complex geometry, however this study involved some limitations. For instance, in the E-Yield simulation, traffic noise is not considered, future work will focus on a real case study, including the simulation and validation of a PV noise barrier with real traffic noise to investigate the effects of vibrations and car turbulence on the PV system's performance and reliability. Moreover, the thermal model input parameters in the E-Yield simulation (thermal resistances, thermal capacitances, and layer thickness) require some adjustment and thorough examination of the heat transfer process, as the current thermal model overestimates cell temperature, as shown in Figure 5 (B).

The acoustic simulation can also be enhanced. In the current simulation, the noise generated by cars is modeled as a unit-amplitude monopole, although traffic noise varies with vehicle type and highway congestion. The wall is also assumed to be rigid. However, minor vibrations, considered negligible, may affect the noise. For the cassette configuration, the fluid resistivity value for Rockwool was taken from the technical data sheet, however, experiments could verify this value to determine the actual fluid resistivity parameter. For the shingles configuration, absorbing boundary conditions were applied based on the absorbing class of the "Faseton Hohlwelle," but as the material's absorption is likely frequency-dependent, future experiments could help determine the frequency-dependent absorption coefficient.

4. Conclusions and Outlook

In this work, a comprehensive energy yield assessment for noise barriers using cassette built-on and shingles built-on designs with a zigzag configuration is conducted. This study examines the PV energy yield and noise reduction efficiency of these two noise barrier designs with a zigzag configuration. Various parameters such the height, PV modules tilt, and cassette/shingle distances are varied to explore their impact on PV energy yield and acoustic pressure received. A case study is evaluated on the European road E19 in Belgium to investigate the effects of these different degrees of freedom on the yearly energy yield and noise reduction capability in the selected location. The results reveal that cassette built-on noise barriers are more effective in energy yield performance due to reflected irradiance from the cassettes. Additionally, they are as efficient as shingles built-on in noise reduction, as the cassettes effectively reflect noise, preventing it from reaching the receptors on the other side. The higher module temperature, due to the noise-absorbing material inside the cassettes, was found to have a minimal effect on power performance. The results also indicate that high-rise noise barriers are better for noise reduction, while they negatively impact energy yield due to shading effects from the overhead cassettes. Hence, a trade-off between the two (moderate height: 6m) can be a solution to this concern. Future work will focus on enhancing the thermal model within the framework to validate the demonstrator's performance. Additionally, we will investigate various types of noise absorbers within the cassettes or attached to the walls to study their impact on PV module temperature and sound pressure levels at the receptor's side. Future studies will also involve testing various types of roads (e.g., asphalt) and examining the impact of albedo on the energy yield for PV noise barriers with different configurations.

Supporting Information

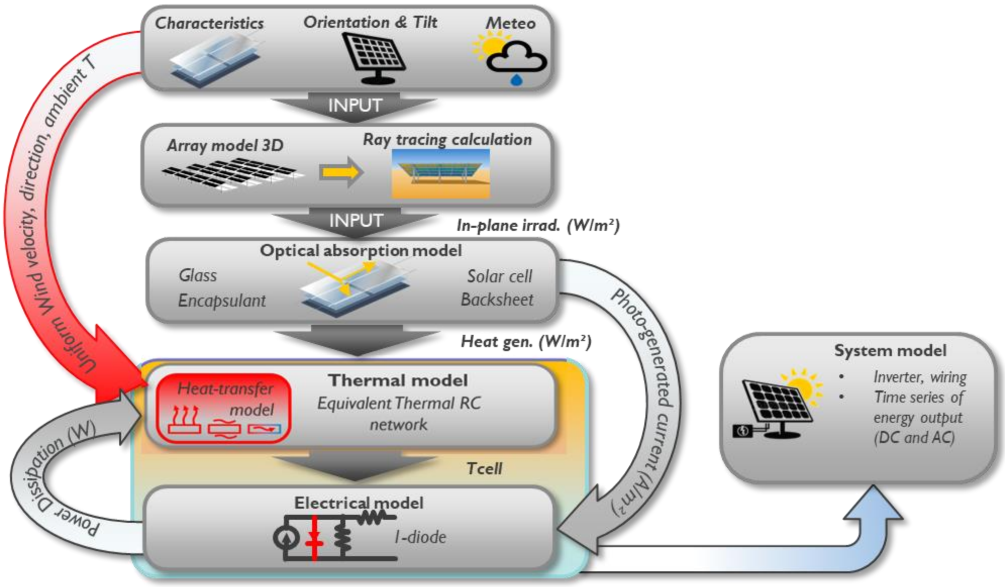

Figure 13 Energy Yield Simulation Framework[14].

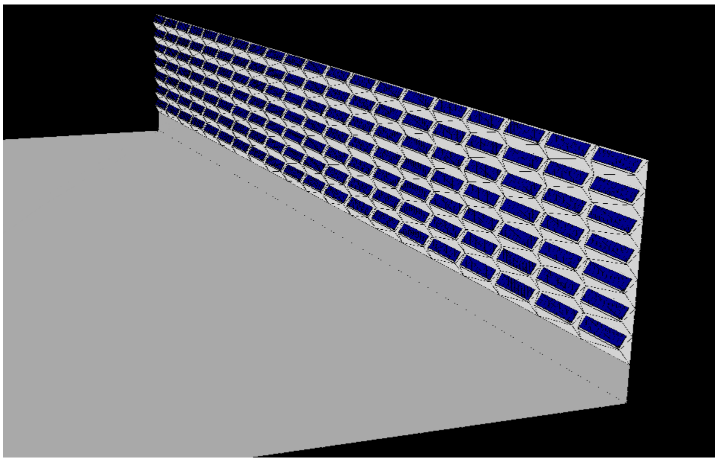

Figure 14 3D model for a 6 m high noise barrier and module tilt of 60° using the scene generator tool.

Table 1 Description of the optical, electrical, and thermal model in the Energy yield framework.

Optical Model	**Electrical Model (Module)**	**Thermal Model**
Aluminum cassettes in S1 and S2: RGB= [0.5176, 0.5294, 0.5373] Specularity: 0.8 Roughness: 0.1 **Ground** RGB= [0.8353, 0.8118, 0.8118] **Noise absorbing material in S3 (Shingles):** RGB=[0.729, 0.667, 0.504]	Peak Power (Pmpp) : 103 Wp Peak Power Voltage (Vmpp) :11.3 V Peak Power Current (Impp) : 9.2 A Open Circuit Voltage (Voc): 13.2 V Short circuit current (Isc) : 9.7 A Maximum System Voltage: 1000 V Limiting reverse current (IR) : 15A Power tolerance = +/- 5%	**Rockwool** Thickness: 0.25 m, Density (ρ): 60 kg/m³ Thermal Resistance (r): 60.0 m·K/W Specific Heat Capacity (c): 1030 J/kg·K **Aluminum** Density (ρ): 2710 kg/m³ Thermal Resistance (r): 0.004 m·K/W Specific Heat Capacity (c): 890 J/kg·K

Figure 15 Location of the case study: E19, Antwerp (51.12°,4.43°).

(A)

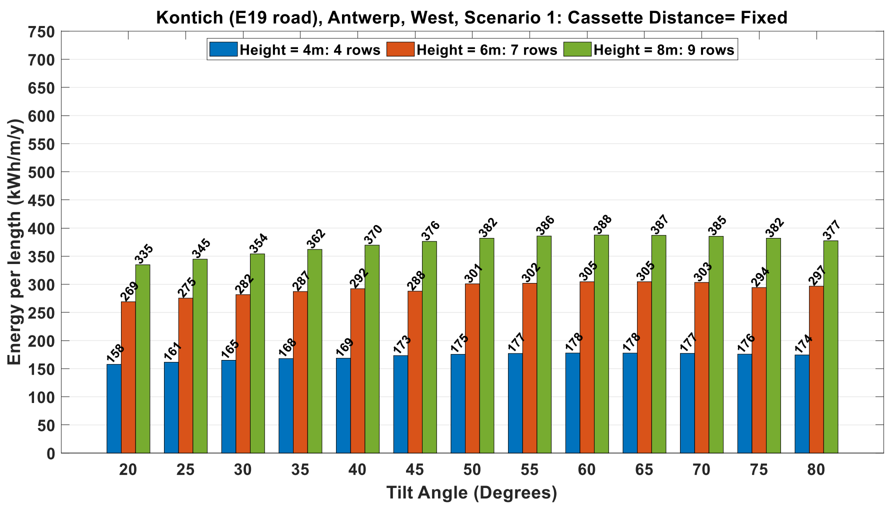

(B)

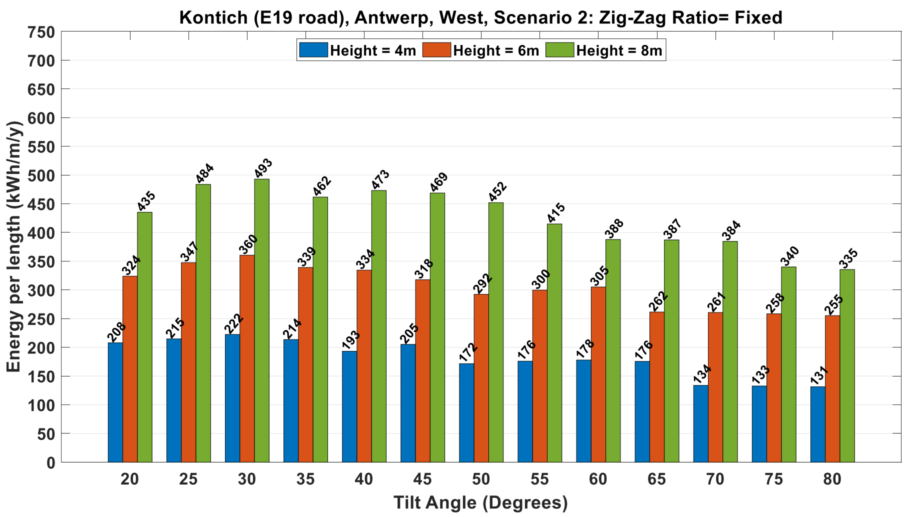

(C)

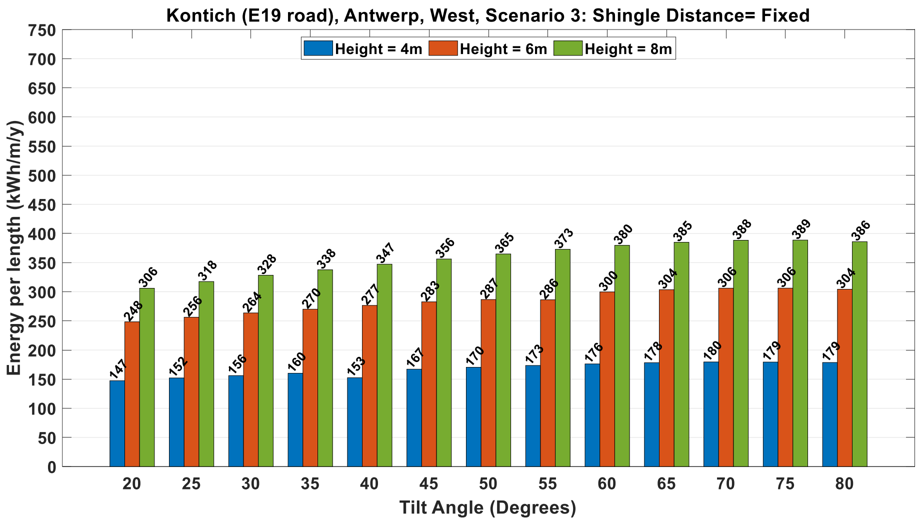

Figure 16 Energy per length for the PV noise barrier in E19 (A) S1 (B) S2 and (C) S3 with west orientation.

(A)

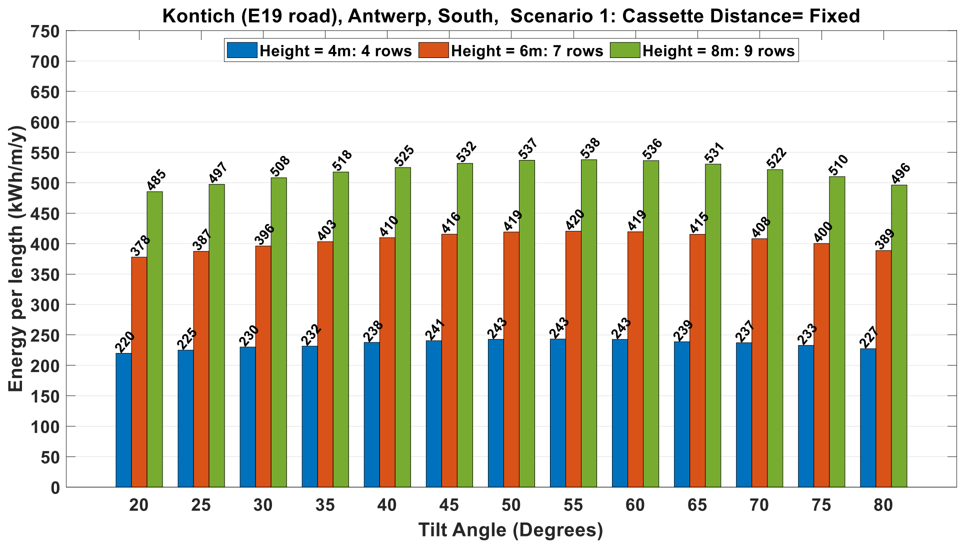

(B)

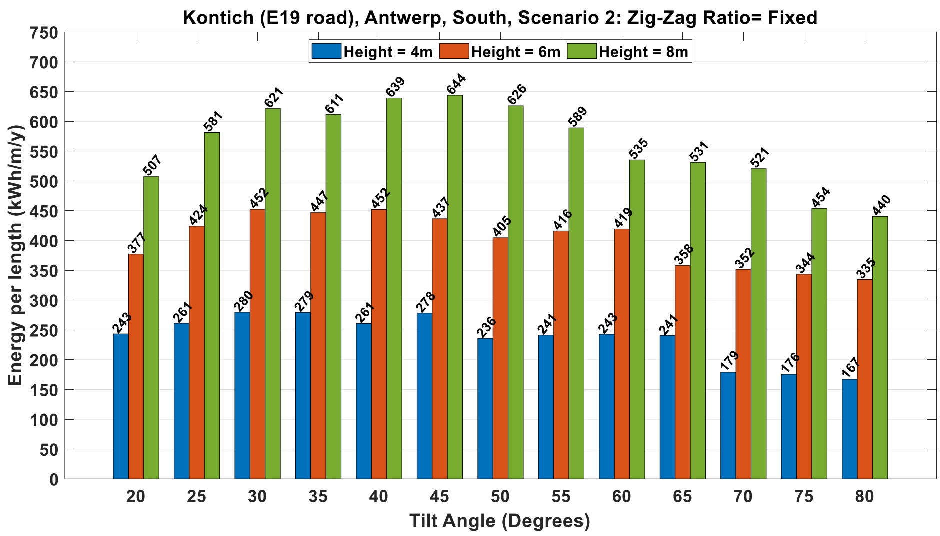

(C)

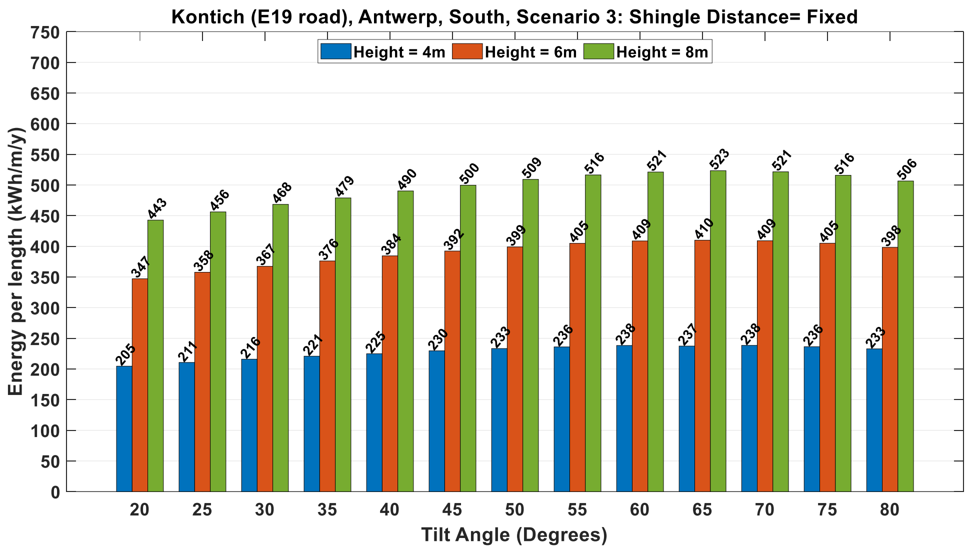

Figure 17 Energy per length for the PV noise barrier in E19 (A) S1 (B) S2 and (C) S3 with South orientation.

(A)

(B)

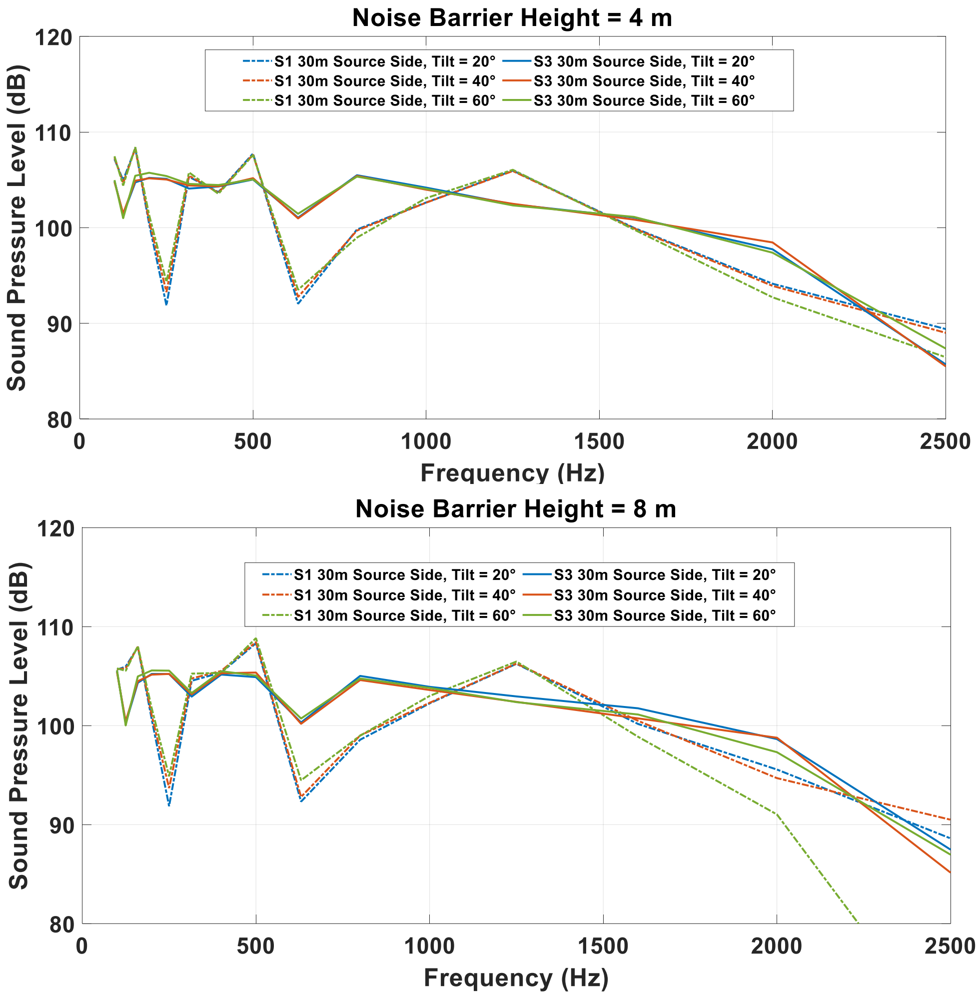

Figure 18 Sound pressure levels recorded by a microphone located at 30m in the source side for (A) 4 m high noise barrier, (B) 8 m high noise barrier.

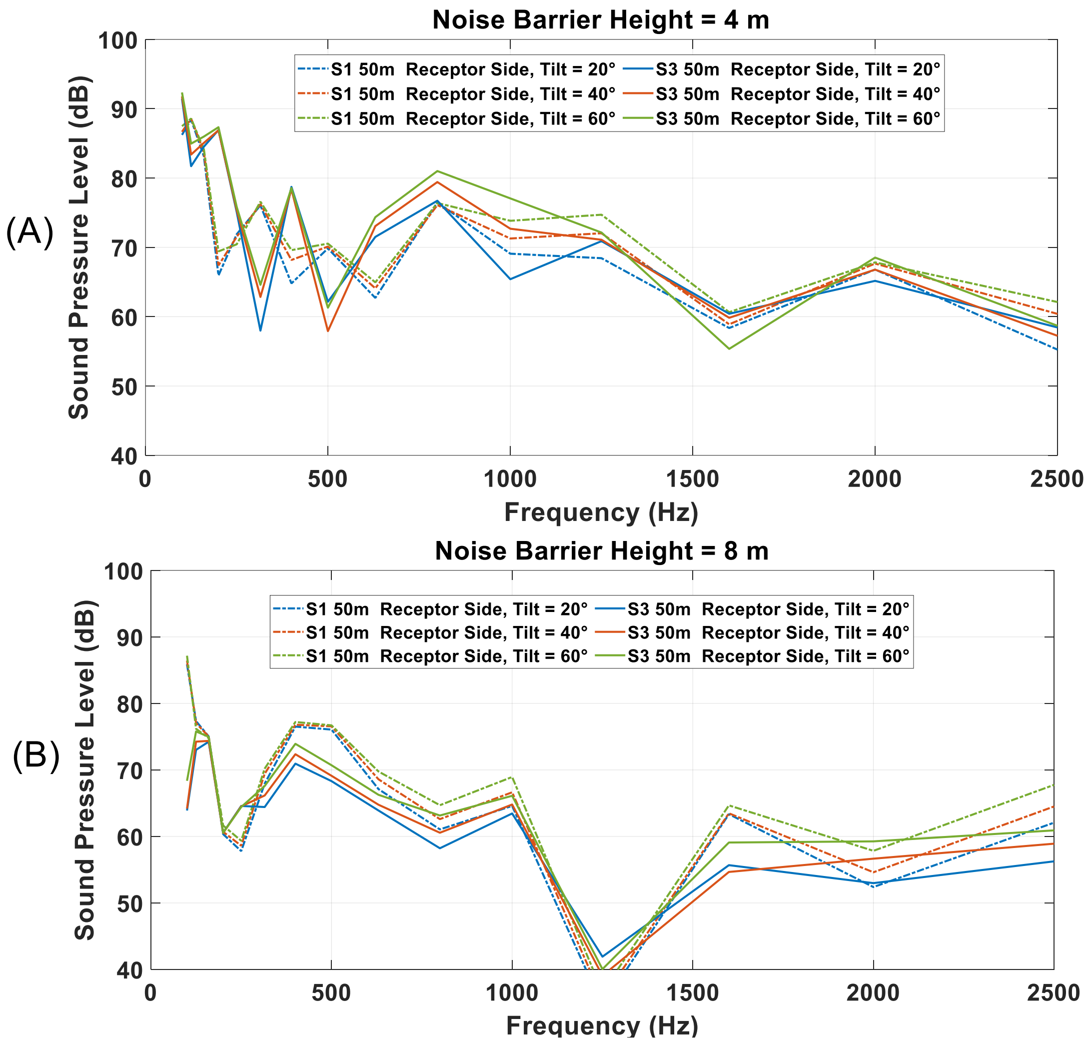

Figure 19 Sound pressure levels recorded by a microphone located at 50m in the receptor side for (A) 4 m high noise barrier, (B) 8 m high noise barrier.

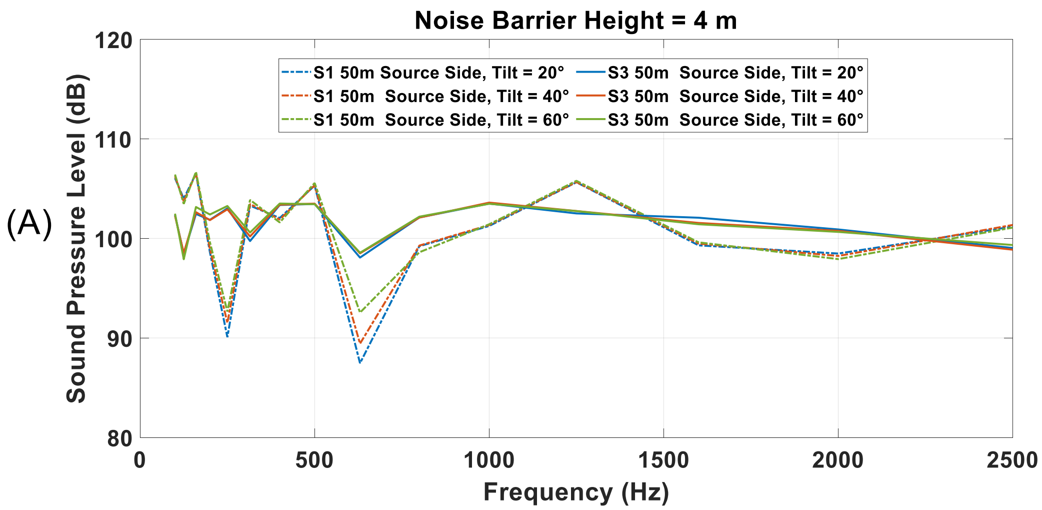

(B)

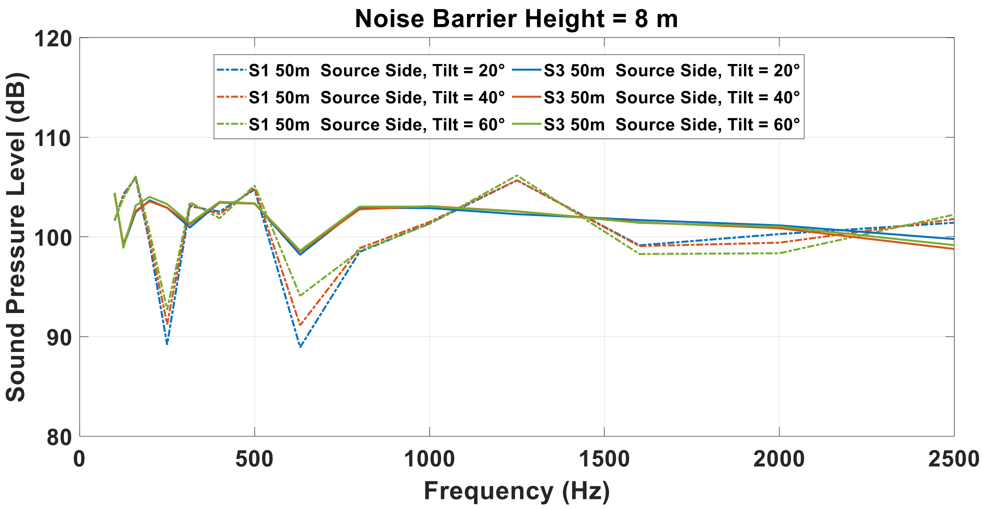

Figure 20 Sound pressure levels recorded by a microphone located at 50m in the source side for (A) 4 m high noise barrier, (B) 8 m high noise barrier.

Acknowledgements

This work is conducted within the Solar Energy Made Regional (SolarEMR) project, within the Interreg V-A Euregio MeuseRhine, with support from the European Regional Development Fund. The authors thank Wim Van De Wall from ZigZagSolar, Eindhoven, Netherlands and Tatjana Vavilki from Soltech, Genk, Belgium.

References

[1] 72% of Belgians live less than 5 kilometres away from a motorway entrance, https://statbel.fgov.be/ (Accessed: May, 2024).
[2] *Highways Department - Guidelines on Design of Noise Barriers*, https://Www.Hyd.Gov.Hk/En/Technical_references/Technical_document/Guidelines_on_noise_barriers/Index.Html (Accessed: June 2024).
[3] L. Clavadetscher, T. Nordmann, in *Sixt. Eur. Photovolt. Sol. Energy Conf.*, Routledge, **2020**, pp. 2249–2252.
[4] C. Poe, A. Plovnick, T. Hodges, A. Hastings, S. Dresley, others, *United States. Federal Highway Administration. Office of Natural Environment* **2017**.
[5] The Declining Cost of Solar Panels, https://www.greenmatch.co.uk/blog/decrease-in-solar-costs/ (Accessed: September 2024).
[6] S. R. Wadhawan, J. M. Pearce, *Renew. Sustain. Energy Rev.* **2017**, *80*, 125.
[7] T. Nordmann, L. Clavadetscher, *Prog. Photovolt. Res. Appl.* **2004**, *12*, 485.
[8] Vertical Solar facade. Your Solar Wall solution, https://www.zigzagsolar.com/ (Accessed: May 2024).
[9] L. Soares, H. Wang, *Transp. Res. Part Transp. Environ.* **2023**, *116*, 103624.
[10] J. Forster, G. Tsutzkiridze, C. Herr, J. Huyeng, F. Basler, R. Kohlhauer, D. H. Neuhaus, M. Heinrich, L. C. Rendler, *40th Eur. Photovolt. Sol. Energy Conf. Exhib.* **2023**, 020439.
[11] SolarEMR, https://www.interregemr.eu/projects/solaremr-en (Accessed: May 2024).
[12] Acoustic Insulation, https://www.rockwool.com/group/products-and-applications/acoustic-insulation/ (Accessed: July 2024).
[13] P. Nivelle, L. Maes, J. Poortmans, M. Daenen, *Prog. Photovolt. Res. Appl.* **2023**, *31*, 173.

[14] I. T. Horváth, H. Goverde, P. Manganiello, J. Govaerts, L. Tous, B. Aldalali, E. Vörösházi, J. Szlufcik, F. Catthoor, J. Poortmans, *Sol. Energy* **2018**, *173*, 728.
[15] RADIANCE WWW server, https://radsite.lbl.gov/radiance/ (Accessed: June 2024).
[16] T. Huld, R. Müller, A. Gambardella, *Sol. Energy* **2012**, *86*, 1803.
[17] Geluid en trillingen | Wegen en verkeer, https://wegenenverkeer.be/ (Accessed: July 2024).
[18] M. Cai, S. Zhong, H. Wang, Y. Chen, W. Zeng, *Appl. Acoust.* **2017**, *123*, 55.
[19] H. Wang, P. Luo, M. Cai, *Appl. Sci.* **2018**, *8*, 100.
[20] P. Ineichen, R. Perez, R. Seal, E. Maxwell, A. Zalenka, *Ashrae Trans* **1992**, *98*, 354.
[21] E. L. Maxwell, *A Quasi-Physical Model for Converting Hourly Global Horizontal to Direct Normal Insolation*, Solar Energy Research Inst., Golden, CO (USA), **1987**.